Elastic modulus of low-k dielectric thin films measured by load-dependent contact-resonance atomic force microscopy

G. Stan,[1][*] S. W. King,[2] and R. F. Cook[1]

[1]*Ceramics Division, National Institute of Standards and Technology, Gaithersburg, Maryland 20899, USA*
[2]*Portland Technology Development, Intel Corporation, Hillsboro, Oregon 97124, USA*

Correlated force and contact-resonance versus displacement responses have been resolved using load-dependent contact-resonance atomic force microscopy (AFM) to determine the elastic modulus of low-k dielectric thin films. The measurements consisted of recording simultaneously both the deflection and resonance frequency shift of an AFM cantilever-probe as the probe was gradually brought in and out of contact. As the applied forces were restricted to the range of adhesive forces, low-k dielectric films of elastic modulus varying from GPa to hundreds of GPa were measurable in this investigation. Over this elastic modulus range, the reliability of load-dependent contact-resonance AFM measurements was confirmed by comparing these results with that from picosecond laser acoustics measurements.

At the core of technology advances in modern nano-electronics is the knowledge and advantageous use of material properties at the nanoscale. Mastering both the electrical *and* mechanical properties of materials has proven to be crucial in successful fabrication of new integrated electronic systems. Since the invention of atomic force microscopy (AFM)[1], interrogation of mechanical properties at the nanoscale for electronics and other technologies has been a propelling factor in developing various dynamic AFM-based techniques: contact-resonance AFM (CR-AFM) (which includes atomic force acoustic microscopy[2] and ultrasonic atomic force microscopy[3]), ultrasonic force microscopy[4], torsional harmonic dynamic force microscopy[5] amongst others.

In this work, we propose a novel procedure for measuring the elastic modulus of nanoscale volumes probed by AFM. The procedure is based on recording real-time contact-resonance frequency versus force curves in the range of small applied contact forces. The benefit of working at small applied forces is that the mechanical properties of materials in the form of samples of reduced thickness (*e.g.*, nanostructures[6] and thin films[7]) can be probed. The drawback is that controlling the applied force in the range of adhesion forces can be a difficult and deceiving task in CR-AFM measurements. However, much of the unknown error can be eliminated when measurements are performed not simply at a single applied force but over a force range, such that the force dependence of contact-resonance frequencies is measured. Moreover, by correlating the measurements on a test material with those on a reference, the need for accurate measurements of some parameters (*e.g.*, cantilever stiffness and tip radius) is eliminated.[8,9]

We have tested the applicability of the proposed method by performing load-dependent CR-AFM measurements on low dielectric constant (low-k) materials: amorphous hydrogenated silicon carbide (a-SiC:H) and oxycarbide (a-SiOC:H) films. Mechanical properties of low-k dielectric films[10,11] are vital for fabricating robust architectures in copper interconnection-based electronics. CR-AFM measurements were made on films of elastic modulus in the range of GPa (compliant materials) to hundreds of GPa (stiff materials) and thickness around 500 nm. The CR-AFM results were compared with those from picosecond laser acoustics (PLA)[12,13] measurements made on samples of the same thickness but larger area.

All films used in these experiments were deposited on 300 mm Si(100) wafers using a high volume manufacturing PECVD system at temperatures on the order of 400 °C. The precursors used for deposition consisted of various combinations of SiH_4, methylsilanes, H_2, He, and oxidizing gases. Young's modulus for these films was first determined by PLA. This ultrasonic technique requires knowledge of the film density as well as Poisson's ratio. The film density for these films was determined using an X-ray reflectivity technique[14] and a Poisson's ratio of 0.25 was assumed. For the SiOC:H films, the presence of porosity was checked using solvent diffusivity measurements described elsewhere.[15] All film deposition and subsequent measurements were performed in high volume manufacturing, class 10 microelectronic fabrication clean rooms with relative humidity controlled to 40 ± 1 %.

CR-AFM exploits the sensitivity of AFM cantilever resonances to the elastic properties of materials probed. The shifts experienced by the resonance frequencies of a cantilever when the AFM probe is brought from air into contact are converted into the elastic modulus of the material tested. First, a clamped-spring coupled beam model[2] is used to determine the contact stiffness from the measured cantilever dynamics and, second, an adequate contact mechanics model is needed to convert contact stiffness into elastic modulus. Nominally, CR-AFM measurements are performed at a fix applied force, a few times greater than the adhesion force between the probe and material. With these precautions, (i) the applied force can be easily controlled with a precision better than 10% even with a stiff cantilever (20 Nm^{-1} to 40 Nm^{-1}) and (ii) the contact can be described by simple contact

mechanics models that neglect the contribution of adhesion forces (*e.g.*, Hertz model[16]). The approach followed in the present work was to measure the contact resonance frequencies while the AFM probe was gradually brought in and out of contact with the sample. In these excursions, the applied force was varied back and forth from the adhesion force - when the contact was first established, to forces about three times the adhesion force (250 nN to 300 nN) - at the maximum applied force.

The force-dependent CR-AFM measurements were accomplished by connecting additional LabVIEW (National Instruments, Austin, TX) instrumentation to a commercial AFM (Veeco MultiMode III, Santa Barbara, CA).[17] Force versus displacement and contact-resonance frequency versus displacement responses were acquired in the following way: at a given tip-sample separation, the AFM z-piezo and low-frequency photodiode voltages were read to determine the position and applied force and then the resonance frequency of the cantilever was identified by sweeping the frequency of the imposed cantilever vibration in the kilohertz to megahertz range. This procedure was repeated at incremental steps of the z-piezo scanner during the approach and retract excursions. An example of such responses is shown in Fig. 1 for an a-SiOC:H film (elastic modulus around 90 GPa). The AFM probes (R150-NCL NanoSensors, Neuchatel, Switzerland)[17] were single-crystal Si cantilevers made with integrated Si tips. The well-defined tip radius of 150 nm was found to provide stable tip-sample contact during measurements. As can be seen in Fig. 1, with the cantilevers (spring constant, k_c, around 30 Nm^{-1}) and modulation amplitude (less than 1 nm) used, the resonance frequencies were sensitive only in the regime of repulsive contact forces but not in the attractive noncontact region.

In the presence of adhesive forces, the elastic deformation experienced by two objects pressed into contact is analytically solved in two limiting cases: the Johnson-Kendall-Roberts (JKR) model,[18] which includes the short-range adhesion between relatively compliant objects with large radii of curvature, and the Derjaguin-Müller-Toporov (DMT) model,[19] which considers the long-range adhesion between relatively stiff objects with small radii of curvature. With either of these models, the quantity needed for interpreting CR-AFM measurements is the normal contact stiffness. In the elastic deformation domain, the normal contact stiffness between two objects in contact is defined as the normal force gradient applied on the contact (the derivative of the normal force acting at the contact with respect to the relative displacement of the objects along the direction of the applied force). Thus, the normal contact stiffness k_n between a spherical tip of radius R_T and a flat surface depends on the applied normal force F_n as

$$k_{n,\text{JKR}} = (6R_T F_n E^{\star 2})^{1/3} \frac{\left(\sqrt{\xi} + \sqrt{1+\xi}\right)^{2/3}}{1 + \frac{2}{3}\sqrt{\xi/(1+\xi)}} \quad (1)$$
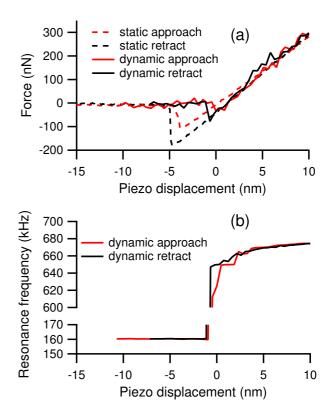

FIG. 1: (a) Static (dashed line) and dynamic (continuous line) force versus displacement responses for an a-SiOC:H film of elastic modulus around 90 GPa. (b) The contact-resonance frequency versus displacement responses were acquired during the dynamic approach and retract excursions shown in (a).

in the JKR model and

$$k_{n,\text{DMT}} = (6R_T F_n E^{\star 2})^{1/3}(1 + \xi)^{1/3} \quad (2)$$

in the DMT model, respectively, with $\xi = F_{ad}/F_n$ being the adhesion force normalized by the applied normal force. In the above equations, the indentation moduli of the tip M_T and sample M_S are included in the reduced elastic modulus, $E^{\star} = 1/(1/M_T + 1/M_S)$. For simplicity, we assume here elastic isotropy, in which case the indentation modulus is simply defined in terms of the Young's modulus E and Poisson's ratio ν, $M = E/(1 - \nu^2)$.

For each tested sample, force-dependent CR-AFM measurements were bracketed by measurements on a reference Si(100) wafer. In addition to force-dependent CR-AFM measurements made on test samples only,[20] the benefit of using the test/reference contact stiffness ratio is that, as can be seen with either (1) or (2), any dependence on the tip radius is eliminated. To calculate the test/reference contact stiffness ratio, a common force range was identified in the retraction stages of the recorded force vs displacement and contact-resonance frequency vs displacement responses on the tested and reference materials. In Fig. 2, this contact stiffness ratio
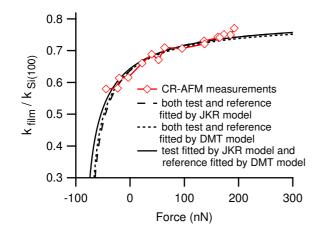
FIG. 2: Force dependence of the contact stiffness on an a-SiOC:H film normalized to the contact stiffness on Si(100). The symbols are the results of force-dependent CR-AFM measurements and the curves represent the fits provided by the DMT and JKR models in various cases. When either the DMT or JKR model was used for both test (a-SiOC:H film) and reference (Si(100)) materials, a good fit was obtained with the following fit parameters: $M_{film} = 90$ GPa, $F_{ad,film} = 70$ nN, $M_{Si(100)} = 165$ GPa, $F_{ad,Si(100)} = 190$ nN. Slightly different fit parameters, $M_{film} = 93$ GPa, $F_{ad,film} = 80$ nN, $M_{Si(100)} = 165$ GPa, $F_{ad,Si(100)} = 190$ nN, generated a good fit in the case when the DMT model was considered for the tip-reference contact and the JKR model for the tip-test contact.

is shown for an a-SiOC:H film and Si(100) at forces less than 200 nN. Over the same force range, equations (1) and (2) were used to calculate the theoretical expressions for the test/reference contact stiffness ratio in the JKR and DMT models, respectively. In the range of small forces considered here, the necessity of acknowledging the contribution of adhesion forces to CR-AFM measurements is motivated by the non-zero values of contact stiffness unmistakably observed at zero applied force.

Good data fits were obtained with both models by adjusting the fit parameters in each case: the indentation modulus of the test material and the adhesion forces at pull-off on the test and reference materials. The fit values of the adhesion forces were found to be closer to the pull-off values measured in the dynamic force-distance curves rather than that observed in their static counterparts. It is conceivable (refer to Fig. 1) that in the dynamic measurements, the mechanical modulation altered the snap-on and pull-off contact forces. Slightly different parameters generated the best fit for two different cases considered (see Fig. 2): (1) either JKR or DMT model for both tip-sample and tip-reference contacts or (ii) JKR model for the tip-sample contact and DMT model for the tip-reference contact. Nominally, only in the case of zero adhesion force,[8,9] does the test/reference contact stiffness ratio eliminate the error introduced by the uncertainty in
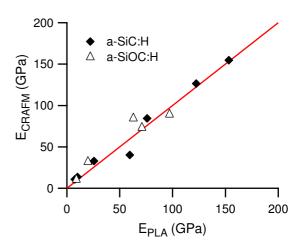

FIG. 3: Elastic modulus as determined from CR-AFM measurements versus elastic modulus as measured by PLA technique.

the cantilever's spring constant k_c. However, even when adhesion forces are considered, the uncertainty in k_c has a minor effect if the test/reference contact stiffness ratio is used. Thus, even a $\pm$ 15 % uncertainty in k_c (a quite large uncertainty) would only introduce an uncertainty of less than $\pm$ 3 % in the calculation of the elastic modulus of the material tested. Relatively small surface roughness (average roughness between 0.4 nm and 0.6 nm) was measured for both a-SiC:H or a-SiOC:H films investigated in this work. As such, the contact mechanics considered was that for smooth surfaces with no surface roughness taken into account for the elastic modulus calculation.[21] No correlations between porosity, surface roughness, and determined elastic modulus were observed.

For each measured low-k thin film, the indentation modulus M determined from CR-AFM measurements was converted into Young's modulus E by using the isotropic relationship, $E = M(1 - \nu^2)$, with a Poisson's ratio $\nu = 0.25$. It is conceivable that small corrections to the Young's modulus calculated in this way would be imposed by a Poisson's ratio that is characteristic of each film. Such corrections could be provided by additional elastic property characterization (e.g., Brillouin light scattering[13]). In Fig. 3 are shown the results of CR-AFM measurements versus PLA over the investigated range of elastic modulus from 10 GPa to 160 GPa. The CR-AFM values were calculated by using the DMT model for both tip-test and tip-reference contacts. Alternatively, when the DMT model was considered for the tip-reference contact and JKR for the tip-test contact, small variations in the fit parameters (within 5 % for the elastic modulus and 10 % for the adhesion force) for compliant materials ($E < 100$ GPa) and almost negligible variations for stiffer materials ($E > 100$ GPa) were observed. By comparing the elastic moduli measured by CR-AFM and PLA, an average value of

$|1 - E_{\mathrm{CR-AFM}}/E_{\mathrm{PLA}}|_{\mathrm{avrg}} = 23\%$ was calculated for their relative deviations. Although based on different physical concepts, CR-AFM and PLA show excellent agreement and assure, in this way, the confidence of using CR-AFM for local elastic modulus measurements on nanometer-sized samples of elastic modulus in the range of GPa to hundreds of GPa.

The CR-AFM approach developed here complements other implemented[5] or proposed[22,23] dynamic tip-sample interaction AFM techniques for quantitative interrogation of nanoscale mechanical properties of compliant materials for advanced electronic and other applications.

---

[1] G Binning, C. F. Quate, and C. Gerber, Phys. Rev. Lett. **56**, 930 (1986).

[2] U. Rabe, K. Janser, and W. Arnold, Rev. Sci. Instrum. **67**, 3281 (1996).

[3] K. Yamanaka and S. Nakano, Japan. J. Appl. Phys. **35**, 3787 (1996).

[4] O. Kolosov and K. Yamanaka, Japan. J. Appl. Phys. **32**, L1095 (1993).

[5] O. Sahin, S. Magonov, C. Su, C. F. Quate, and O. Solgaard, Nature Nanotech. **2**, 507 (2007).

[6] G. Stan, S. Krylyuk, A. Davydov, M. Vaudin, L. A. Bendersky, and R. F. Cook, Appl. Phys. Lett. **92**, 241908 (2008).

[7] G. Stan and R. F. Cook, Nanotechnology **19** 235701 (2008).

[8] U. Rabe, S. Amelio, M. Kopycinska, S. Hirsekorn, M. Kempf, M. Goken, and W. Arnold, Surf. Interface. Anal. **33**, 65 (2002).

[9] D. C. Hurley, K. Shen, N. M. Jennett, and J. A. Turner, J. Appl. Phys. **94**, 2347 (2003).

[10] L. Wang, M. Ganor, S. I. Rokhlin, A. Grill, J. Mater. Res. **20**, 2080 (2005).

[11] D. J. Morris and R. F. Cook, J. Mater. Res. **23**, 2429 (2008).

[12] G. A. Antonelli, B. Perrin, B. C. Daly, and D.G. Cahill, MRS Bull. **31**, 607 (2006).

[13] A. Link, R. Sooryakumar, R. S. Bandhu, G. A. Antonelli, J. Appl. Phys. **100**, 013507 (2006).

[14] E. Chason and T. M. Mayer, Crit. Rev. Sol. Stat. Mat. Sci **22**, 1 (1997).

[15] M. A. Worsley, M. Roberts, S. F. Bent, S. M. Gates, T. Shaw, W. Volksen, R. Miller, Microelectron. Eng. **82**, 113 (2005).

[16] K. L. Johnson, *Contact Mechanics* (Cambridge University Press, Cambridge, 1996).

[17] Any mention of commercial products in this article is for information only; it does not imply recommendation or endorsement by the NIST.

[18] K. L. Johnson, K. Kendall, and A. D. Roberts, Proc. R. Soc. London A **324**, 301 (1971).

[19] B. V. Derjaguin, V. M. Müller, and Y. P. Toporov, J. Colloid Interf. Sci. **53**, 314 (1975).

[20] M. Kopycinska-Müller, R. H. Geiss, D. C. Hurley, Ultramicroscopy **106**, 466 (2006).

[21] A. Vincent, S. Babu and S. Seal, Appl. Phys. Lett. **91**, 161901 (2007).

[22] M. Balantekin, A. G. Onaran, and F. L. Degertekin, Nanotechnology **19**, 085704 (2008).

[23] S. D. Solares and G. Chawla, Meas. Sci. Technol. **19**, 055502 (2008).